PCCP

PAPER

View Article Online
View Journal | View Issue

Cite this: *Phys. Chem. Chem. Phys.*, 2022, **24**, 4843

The kinetics of the reactions of Br atoms with the xylenes: an experimental and theoretical study†

Binod R. Giri, *[a] Aamir Farooq, [a] Milán Szőri [b] and John M. Roscoe *[c]

This work reports the temperature dependence of the rate coefficients for the reactions of atomic bromine with the xylenes that are determined experimentally and theoretically. The experiments were carried out in a Pyrex chamber equipped with fluorescent lamps to measure the rate coefficients at temperatures from 295 K to 346 K. Experiments were made at several concentrations of oxygen to assess its potential kinetic role under atmospheric conditions and to validate comparison of our rate coefficients with those obtained by others using air as the diluent. Br_2 was used to generate Br atoms photolytically. The relative rate method was used to obtain the rate coefficients for the reactions of Br atoms with the xylenes. The reactions of Br with both toluene and diethyl ether (DEE) were used as reference reactions where the loss of the organic reactants was measured by gas chromatography. The rate coefficient for the reaction of Br with diethyl ether was also measured in the same way over the same temperature range with toluene as the reference reactant. The rate coefficients were independent of the concentration of O_2. The experimentally determined temperature dependence of the rate coefficients of these reactions can be given in the units cm^3 $molecule^{-1}$ s^{-1} by: *o*-xylene + Br, $\log_{10}(k) = (-10.03 \pm 0.35) - (921 \pm 110)/T$; *m*-xylene + Br, $\log_{10}(k) = (-10.78 \pm 0.09) - (787 \pm 92/T)$; *p*-xylene + Br, $\log_{10}(k) = (-9.98 \pm 0.39) - (956 \pm 121)/T$; diethyl ether + Br, $\log_{10}(k) = (-7.69 \pm 0.55) - (1700 \pm 180)/T$. This leads to the following rate coefficients, in the units of cm^3 $molecule^{-1}$ s^{-1}, based on our experimental measurements: *o*-xylene + Br, $k(298\ K) = 7.53 \times 10^{-14}$; *m*-xylene + Br, $k(298\ K) = 3.77 \times 10^{-14}$; *p*-xylene + Br, $k(298\ K) = 6.43 \times 10^{-14}$; diethyl ether + Br, $k(298\ K) = 4.02 \times 10^{-14}$. Various *ab initio* methods including G3, G4, CCSD(T)/cc-pV(D,T)Z//MP2/aug-cc-pVDZ and CCSD(T)/cc-pV(D,T)Z//B3LYP/cc-pVTZ levels of theory were employed to gain detailed information about the kinetics as well as the thermochemical quantities. Among the *ab initio* methods, the G4 method performed remarkably well in describing the kinetics and thermochemistry of the xylenes + Br reaction system. Our theoretical calculations revealed that the reaction of Br atoms with the xylenes proceeds *via* a complex forming mechanism in an overall endothermic reaction. The rate determining step is the intramolecular rearrangement of the pre-reactive complex leading to the post-reactive complex. After lowering the relative energy of the corresponding transition state by less than 1.5 kJ mol^{-1} for this step in the reaction of each of the xylenes with Br, the calculated rate coefficients are in very good agreement with the experimental data.

Received 14th August 2021,
Accepted 14th January 2022

DOI: 10.1039/d1cp03740d

rsc.li/pccp

1. Introduction

The importance of reactions of atomic halogens to the chemistry of the atmosphere has been recognized for a long time. On the subject, recent reviews[1,2] provide a rich source of citations of the primary literature. The reactions of Cl, OH and Br are potentially involved in the photo-oxidation of volatile organic compounds (VOCs) in the atmosphere and have some similarities as well as significant differences in their reactivity. There are several extensive compilations of kinetic data for these reactions[3–6] which lead to the generalization that, for the most part, reactions of Cl with saturated VOCs are faster than the corresponding reactions of OH which are faster than those of Br. Much of the kinetic data for reactions of Cl and Br have been obtained at temperatures close to 300 K. However, in those cases in which the dependence of the rate coefficients on temperature has been examined directly, reactions of Cl atoms with saturated VOCs

[a] *King Abdullah University of Science and Technology (KAUST), Clean Combustion Research Center, Division of Physical Sciences and Engineering, Thuwal 23955-6900, Saudi Arabia. E-mail: binod.giri@kaust.edu.sa*
[b] *Institute of Chemistry, Faculty of Materials Science and Engineering, University of Miskolc, Egyetemváros A/4, H-3515 Miskolc, Hungary*
[c] *Department of Chemistry, Acadia University, Wolfville, Nova Scotia, B4P 2R6, Canada. E-mail: john.roscoe@acadiau.ca*

† Electronic supplementary information (ESI) available. See DOI: 10.1039/d1cp03740d

take place with little or no activation energy. It was found that the reactions of Cl atoms with saturated VOCs are of the order of 10^{-10} cm^3 molecule^{-1} s^{-1}, approaching the collision-controlled limit. However, the reactions of OH and Br with saturated VOCs exhibit a wide variation of reactivity displaying non-Arrhenius behavior.

It is well-known that the reactions of important atmospheric species (X = OH, Cl and Br) with oxygenated volatile organic compounds (OVOCs, denoted as RH) or aromtics take place in a multistep mechanism *via* complex formation at the entrance and exit channels as outlined below.[7–16] Here, RH is an OVOC such as an ether or an alcohol. The first step is the barrierless, reversible formation of a pre-reactive addition complex, RH···X, in an exothermic process.

$$RH + {}^{\bullet}X \rightleftharpoons RH\cdots X \quad \text{(R1a,R-1a)}$$

$$RH\cdots X \rightarrow R\cdots HX \quad \text{(R1b)}$$

$$R\cdots HX \rightarrow R^{\bullet} + HX \quad \text{(R1c)}$$

The second step (R1b) represents an intramolecular hydrogen abstraction of RH···X forming a pre-dissociation complex, R···HX, in which formation of the new H–X polar covalent bond is well advanced and the original R–H covalent bond mainly transforms to a dipole–dipole interaction. This process occurs over a potential barrier, the height of which depends upon the type of an atom or a radical involved in the hydrogen abstraction reaction. The third step is the loose dissociation pathway of R···HX forming HX and an organic free radical, R$^{\bullet}$. This mechanistic picture is consistent with our recent works[7–11] and other *ab initio* studies for reactions of halogen atoms with organic compounds.[12,17–20]

We have undertaken a research program over several years to investigate the temperature dependence of reactions of Cl and Br with VOCs to rationalize the differences in their reaction mechanisms.[7,8,10,11,21–24] The interpretation of the results has been assisted by using *ab initio* methods to explore the plausible reaction pathways on the potential energy surfaces. Unlike Cl atoms, Br atoms often display an interesting reactivity behavior with VOCs. For the reactions of Br with VOCs, a large variation in the enthalpy of activation and entropy of activation is observed (see Giri *et al.*[23]). Such variation mainly stems from the structural differences in the transition states of the reactions of Br atoms with structurally similar VOCs. All the hydrogen abstraction reactions from VOCs by Br atoms are endothermic overall and display a significant activation energy, whereas they are exothermic for reactions of Cl with VOCs with some exceptions (*e.g.* $C_6H_6 + Cl \rightarrow C_6H_5 + HCl$ [$\Delta_{rxn,298K}H^{\circ}$ = 51.4 kJ mol^{-1} at the CCSD(T)/aug-cc-pVDZ//PBE0/aug-pc1 level of theory][25]). For these reactions under atmospheric conditions, the entrance channel generally governs the kinetics yielding rate coefficients close to the collision limit. For the Cl + VOCs reaction systems, the kinetically relevant inner transition states and the products lie below the reactants' energies. The energies of the pre-dissociative states, R–HCl, are much more negative than the energies of the initial RH···Cl adducts as might be expected since the pre-dissociative states should resemble the products in these exothermic reactions (see Giri *et al.*[8] and Jodkowski *et al.*[12]). Note that the hydrogen abstraction reaction of Cl atoms with saturated hydrocarbons is nearly a barrierless process and can occur directly without intermediates.[19] These discussions account for the lack of temperature dependence for the rate coefficients in the reactions of Cl with VOCs.

Table 1 Rate coefficients at 300 K for reactions of toluene and the xylenes with Br, Cl and OH

Reaction	k(300 K) (cm^3 molecule^{-1} s^{-1})	Ref.
Toluene + Br → products	$(1.6 \pm 0.2) \times 10^{-14}$	This work
Toluene + Br → products	$(1.3 \pm 0.2) \times 10^{-14}$	26
o-Xylene + Br → products	$(7.9 \pm 0.9) \times 10^{-14}$	This work
o-Xylene + Br → products	$(8.9 \pm 1.8) \times 10^{-14}$	26
m-Xylene + Br → products	$(4.0 \pm 0.4) \times 10^{-14}$	This work
m-Xylene + Br → products	$(6.6 \pm 1.3) \times 10^{-14}$	26
p-Xylene + Br → products	$(6.8 \pm 0.6) \times 10^{-14}$	This work
p-Xylene + Br → products	$(9.0 \pm 1.8) \times 10^{-14}$	26
Toluene + Cl → products	$(5 \pm 1) \times 10^{-11}$	21
o-Xylene + Cl → products	$(1.4 \pm 0.3) \times 10^{-10}$	21
m-Xylene + Cl → products	$(1.4 \pm 0.3) \times 10^{-10}$	21
p-Xylene + Cl → products	$(1.4 \pm 0.3) \times 10^{-10}$	21
Toluene + OH → products	5.63×10^{-12}	27
o-Xylene + OH → products	$(1.19 \pm 0.07) \times 10^{-11}$	28
m-Xylene + OH → products	$(2.14 \pm 0.14) \times 10^{-11}$	28
p-Xylene + OH → products	$(1.19 \pm 0.07) \times 10^{-11}$	28

Recently, we reported experimental results for the temperature dependence of the reactions of Cl with the xylenes and toluene[21] and of toluene with Br.[23] These results along with the literature data for the reactions of Cl, Br and OH with toluene and the xylenes are compiled in Table 1. The rate coefficients for the reactions of Cl with toluene and the xylenes showed no statistically significant dependence on temperature and were of a very similar magnitude to the rate coefficients of other reactions of Cl with VOCs revealing that the barrierless addition in the entrance channel is the rate determining step. As expected, the rate coefficients for the Cl atom reactions with toluene and the xylenes are close to the collision limit (approximately $\sim 10^{-10}$ cm^3 molecule^{-1} s^{-1}). The rate coefficients for the reactions of Cl with the xylenes were also independent of the xylene isomer, giving an average value of $(1.4 \pm 0.3) \times 10^{-10}$ cm^3 molecule^{-1} s^{-1} at 298 K while the rate coefficient for the reaction of Cl with toluene was $(5.0 \pm 0.6) \times 10^{-11}$ cm^3 molecule^{-1} s^{-1}. Here, the difference in reactivity of Cl with toluene and the xylenes stems from the difference in the statistical factor. On the contrary, the reactions of Br and OH with these aromatics display some variations in their reactivity. Such behavior may be largely due to the variation of the potential barrier of reaction step (R1b) along the reaction pathway. Therefore, the aims of this study are:

(i) Determine the temperature dependence of the reactions of the xylenes with atomic bromine experimentally.

(ii) Employ various *ab initio* methods to fully characterize the potential energy surfaces by exploring all the plausible pathways for the reactions of the xylenes with Br. This will help to rationalize the appropriateness of various quantum methods to accurately describe the current reaction systems with reliable kinetic and thermodynamic properties.

(iii) The role of RH···X (X = OH) is critical for understanding the low temperature kinetics.[15,29,30] This study will discern the

role of the pre-reactive complex in the dynamics of the reactions of Br atoms with the xylenes and/or similar reactions.

2. Methodology

2.1 Experimental section

Details of the experiments have been described in earlier publications.[11,23,24] Reaction mixtures were prepared in a 70-L Pyrex chamber surrounded by four 40 W fluorescent lamps with useful output from 350 to 650 nm. Atomic bromine was produced by photolysis of Br_2. The concentrations of the organic reactants ranged from 10^{14} to 10^{16} molecules cm^{-3} and the concentration of Br_2 was typically 5 to 10 times larger than the total concentration of the organic reactants to provide efficient scavenging of the free radical products. The chamber was brought to the desired final pressure by adding argon and oxygen. The precision of the concentrations of the components of the reaction mixtures was limited by the precision of the pressure measurements and was typically approximately ±2%. As described in our earlier work, the concentration of Br was estimated from pseudo-first order loss of the organic reactants to be approximately 10^{11} to 10^{12} atoms cm^{-3}.

Pressures in the reaction vessel were measured with a 1000 torr piezoelectric pressure gauge and a 10 torr Baratron pressure gauge (1 torr = 133.32 Pa) to a precision of approximately ±1% of the full-scale reading. While most of the experiments were made at a pressure close to atmospheric, a few experiments were made at lower pressures to determine the effect of pressure on the rate coefficients being measured. The range of pressures accessible in our apparatus was approximately 100 kPa to 27 kPa.

The temperature was varied by circulating heated air around the reaction vessel. The temperature was measured with a calibrated type J thermocouple to within ±0.1 °C and controlled by an Antunes temperature controller to a comparable level of precision. The concentrations of the organic reactants were measured with a gas chromatograph using a flame ionization detector. The analytes were separated on a stainless steel $8' \times 1/8''$ column packed with 80/100 mesh Chromosorb 101. The reaction chamber was connected to the sample loop of the gas chromatograph which allowed direct injection of samples of known pressure. Both the area and the height of the chromatographic peaks were verified to be linear functions of the concentration of the analyte. The numerical values of the concentrations of the organic reactants are not required for the kinetic analysis using the relative rate method. The linear relation between chromatographic signal and concentration of the analyte allows the chromatographic signal to be used directly. This is explained in more detail below. The precision of the signal varied with the magnitude of the concentration being measured but was typically between about ±1% for large concentrations early in a reaction and ±10% for smaller concentrations late in the reaction.

The kinetic analysis is based on the following reactions:

$$RH_{test} + Br^{\bullet} \rightarrow R^{\bullet}_{test} + HBr \quad (R2)$$

$$RH_{ref} + Br^{\bullet} \rightarrow R^{\bullet}_{ref} + HBr \quad (R3)$$

where RH_{test} is the organic reactant whose rate coefficient is to be measured and RH_{ref} is the reference organic reactant. The relative rate analysis requires that reactions (R2) and (R3) are the only loss routes for the organic reactant and that neither organic reactant is regenerated in the overall reaction system. When these constraints are obeyed, the rate coefficients for these reactions are related to the concentrations of the organic reactants by eqn (1)

$$\ln\left\{\frac{[RH_{test}]_0}{[RH_{test}]_t}\right\} = \frac{k_{R2}}{k_{R3}}\ln\left\{\frac{[RH_{ref}]_0}{[RH_{ref}]_t}\right\} \quad (1)$$

A plot of $\ln\{[RH_{test}]_0/[RH_{test}]_t\}$ against $\ln\{[RH_{ref}]_0/[RH_{ref}]_t\}$ is linear with slope k_{R2}/k_{R3} and an intercept of zero. The value of the rate coefficient k_{R2} can then be calculated from the slope of such a plot and the known value of the rate coefficient, k_{R3}, of the reference reaction.

The best precision is obtained if k_{R2} and k_{R3} have similar values. If this is not the case, the analytical precision of the concentration ratio for the slower reaction will be poor because the smaller change in concentration of the organic reactant will be more difficult to measure. This results in a more uncertain value of the rate coefficient ratio. In our experiments, the rate coefficient ratio when toluene was the reference reactant was between 2 and 6. The rate coefficient for the reference reaction[23] had a standard deviation of approximately 10% over the temperature range of its measurement.

When using the relative rate method, it is desirable to measure the rate coefficients for a reaction against more than one reference reaction to evaluate the possibility that the reference reaction might interfere with the kinetics of the reaction whose rate coefficient is to be measured. This also reduces the possibility that an undetected discrepancy in the reference rate coefficient would affect the accuracy of the rate coefficient being measured. The ratio of rate coefficients when diethyl ether was the reference reactant was between 0.5 and 2. We measured the rate coefficient of the reaction of Br with diethyl ether earlier[24] but at that time there were fewer reports of rate coefficients for reactions of Br as a function of temperature. The best reference reaction we could find, which had been measured over a range of temperatures, was the reaction of Br with iso-octane and the rate coefficient ratios ranged from 6 to 14. We decided to remeasure the rate coefficient for the reaction of Br with diethyl ether in the current work, using toluene as the reference, since the indication was that the rate coefficient ratios would be significantly smaller. This should result in better precision for the rate coefficient of the reaction of Br with diethyl ether. The results are reported later in this paper, but it may be mentioned here that the rate coefficient ratios were smaller by approximately a factor of 2, and the precision of the experimental results was somewhat improved. The numerical results for these new measurements were in good agreement with the previous results although the lower temperature measurements gave rate coefficients that were noticeably smaller than those of our earlier work by as much as 20%.

It is important to verify that the measured kinetic data reflect only the reactions of interest and are independent of other aspects of the experiments. We tested the possibility that irradiation of the reactants by the fluorescent lamps might result in their decomposition. Mixtures with concentrations typical of those used in the kinetic experiments were prepared without bromine and were irradiated for periods of time that were longer than the duration of the actual kinetic experiments with bromine. There was no measurable loss of the organic reactants. Similarly, typical reaction mixtures including bromine that stood in the dark over-night in the reaction chamber gave kinetic results that were identical to those that were obtained in experiments made after allowing the reaction mixture to equilibrate in the dark for only half an hour.

Many reports of the kinetics of reactions of organic compounds with Br have used air as the diluent in the reaction mixtures, partly so the large concentration of O_2 would scavenge free radicals generated in the reaction of Br with the organic reactant. In contrast, most of our experiments were made in argon with no added oxygen and a significant excess concentration of Br_2 was provided to scavenge free radicals. This was done to keep the reaction mixture being analyzed as simple as possible, giving fewer peaks in the gas chromatograms. We made several experiments in the presence of O_2 to verify that it had no effect on the numerical values of the rate coefficients being measured. The concentration of O_2 ranged from approximately 7×10^{17} molecules cm^{-3} to 2×10^{19} molecules cm^{-3} which is significantly larger than the concentration of O_2 in air. The addition of O_2 to the reaction mixture slowed the consumption of the organic reactants measurably. However, as in our previous experiments, the addition of O_2 even at concentrations greater than that in air had no effect on the rate coefficient ratios. The effect of O_2 was to slow the reactions of the test reactant and the reference reactant in the same proportion so that there was no measurable effect on the ratio of the rate coefficients. The effect of O_2 is illustrated in Fig. 1. This effect results from competition by O_2 with the reaction of Br_2 with the free radical products (reaction (R4) below) which regenerates Br. This decreases the concentration of Br and consequently extends the reaction over a longer time period which decreases the slopes of the first order plots while leaving the slopes of the relative rate plots unchanged.

$$RH + Br^{\bullet} \rightarrow R^{\bullet} + HBr \quad (R4)$$

$$R^{\bullet} + Br_2 \rightarrow RBr + Br^{\bullet} \quad (R5)$$

$$R^{\bullet} + O_2 \rightarrow RO_2^{\bullet} \rightarrow \text{Products} \quad (R6)$$

The organic reactants used in these experiments were toluene (Sigma-Aldrich; 99.8%, anhydrous), *o*-xylene (Sigma-Aldrich; Chromosolv Plus, for HPLC, 98%), *m*-xylene (Sigma-Aldrich; anhydrous, 99+%), *p*-xylene (Sigma-Aldrich; anhydrous, 99+%), and diethyl ether (ACP; A.C.S. Reagent, anhydrous, >99.0%). These were thoroughly degassed, distilled to the desired partial pressures in their storage bulbs, and brought to atmospheric pressure with argon. Bromine (Sigma-Aldrich; A.C.S. Reagent, >99.5%) was condensed in a cold finger, degassed, distilled to the required partial pressure in its storage bulb, and brought to atmospheric pressure with argon. Oxygen (Praxair; 99.9995%), argon (Praxair; 99.9995%) and the gases used for gas chromatography, helium (Praxair; 99.9995%), medical air (Praxair) and hydrogen (Praxair; 99.95%) were used without further purification.

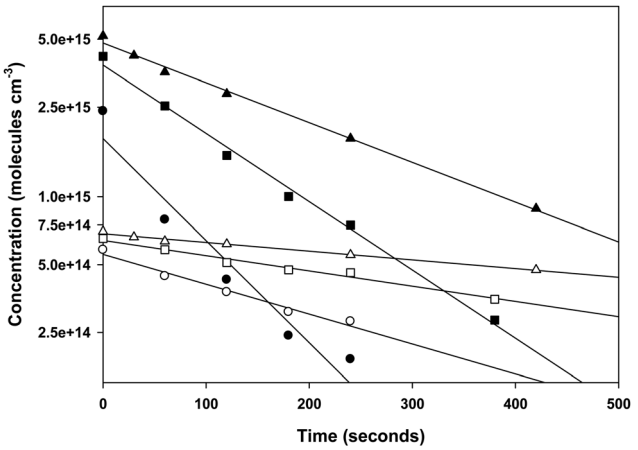

Fig. 1 First order plots of *o*-xylene and toluene at 296 K, 101 kPa total pressure, and different concentrations of O_2. Filled symbols are *o*-xylene and open symbols are toluene. Concentration units are molecules cm^{-3}. (●, ○) $[Br_2] = 1.07 \times 10^{16}$, [*o*-xylene] = 2.47×10^{15}, [toluene] = 5.98×10^{14}, no O_2; (■, □) $[Br_2] = 1.35 \times 10^{16}$, [*o*-xylene] = 4.31×10^{15}, [toluene] = 6.71×10^{14}, $[O_2] = 7.18 \times 10^{17}$; (▲, Δ) $[Br_2] = 1.27 \times 10^{16}$, [*o*-xylene] = 5.32×10^{15}, [toluene] = 7.22×10^{14}, $[O_2] = 3.75 \times 10^{18}$.

2.2 Computational details

Structures and energies. As reported previously,[9] the reactive potential energy surfaces (PES) of bromine-containing systems can show significant method dependence. Therefore, several quantum chemical approaches were employed to characterize the PES of the reactions of Br atoms with the xylenes. First of all, the PES of the *o*-, *m*- and *p*-xylenes with Br atoms were explored using G3[31] and G4[32] composite methods. Note that more sophisticated composite methods such as CBS-APNO and Weizmann-1 are not applicable to Br-containing systems because of the limitations on the basis sets for Br containing chemical systems. In the G3 and G4 methods, the final geometry optimizations were obtained at the MP2/6-31G(d) and B3LYP/6-31G(2df,2p) levels of theory, respectively. To assess the basis set dependency, further optimizations of all species were carried out at the second-order Møller–Plesset (MP2)[33] perturbation theory and Becke-3 Parameter Lee–Yang–Parr (B3LYP) functional[34–36] using Dunning's correlation – consistent double-ζ and triple-ζ basis sets[37,38] by applying the tight convergence criterion. Vibrational analyses were carried out to confirm the identity of the species on the PES. For instance, each of the optimized transition states (TS) has one imaginary frequency corresponding to the reaction coordinate. Using the CCBDB database,[39] the harmonic frequencies obtained at B3LYP/cc-pVTZ and MP2/aug-cc-pVDZ levels of theory were scaled by a factor of (0.970 ± 0.026) and (0.959 ± 0.031), respectively. The scaled vibrational frequencies were used to compute the rate coefficients and the thermodynamic properties.

The intrinsic reaction coordinate (IRC) calculations[40] were performed at the MP2/cc-aug-pVDZ level of theory in both directions. Such calculations for the minimum energy pathway (MEP) confirmed the identity of the TS by appropriately connecting the pre- and post-reactive complexes (noted as RC and PC, respectively).

Using the optimized structures at the MP2/aug-cc-pVDZ and B3LYP/cc-pVTZ levels of theory, we further refined the single-point energies by employing coupled-cluster calculations with single and double excitations[41,42] including the perturbative estimate of the triples contribution (CCSD(T)).[43] As in our toluene + Br work,[9] we carried out a two-point extrapolation scheme, as suggested by Martin[44] and by Feller and Dixon,[45] to obtain CCSD(T) energies at the infinite-basis-set limit: $E_\infty = E_{l\max} - B/(l_{\max} + 1)^4$. Here, $l_{\max}$ is the maximum angular momentum in the cc-pVXZ (X = D, T)[37,38,46] basis sets, and B is a fitting parameter. Such extrapolated CCSD(T) energies at the infinite-basis-set limit can also be denoted as the CCSD(T)/cc-pV(D,T)Z level of theory. We performed T_1 diagnostics[47] to estimate the contribution of higher excitations. For all species, T_1 values were less than 0.03 suggesting that the xylenes + Br system is dominated by dynamical correlations.[47] Therefore, we expect that the CCSD(T)/cc-pV(D,T)Z level of theory can provide an accurate energetic description of the Br atom reactions with the xylenes. We obtained the standard enthalpy of formation ($\Delta_{f,0K}H^\circ$ and $\Delta_{f,298.15K}H^\circ$ at 0 and 298 K, respectively) by means of an atomization scheme (AS). For the essential highly accurate atomization enthalpies, we adopted Ruscic's Active Thermochemical Tables (ATcT).[48] We checked the appropriateness of the model chemistry by comparing directly with the ATcT[48] and Burcat[49] databases. All calculations were performed by using the Gaussian09 software package.[50] The results of the electronic structure calculations (derived molecular parameters, optimized geometrical parameters) are provided in Tables S1–S6 of the ESI.†

Kinetic analysis. As with the toluene + Br reaction,[9] the Br atom reacts with the xylenes *via* a complex formation mechanism as shown in the reaction sequence (R1a)–(R1c) in an overall endothermic process. The formation of a pre-reactive complex (RH···X) constitutes the initial step of a multistep mechanism, whereas the transition state linking the pre-reactive complex (RH···X) with the post-reactive complex (R···HX) lies at the highest energy along the path of the reaction sequence (R1a)–(R1c). The energetics of the reaction will be discussed later. Based on the potential energy profile, a pre-equilibrium arises between the reactants (RH = xylene and X = Br) and the pre-reactive complex (RH···X = xylene···Br) before HBr elimination occurs *via* a tight transition state. In such a case, the overall rate coefficient ($k_{ov.}$) can be reasonably approximated by eqn (2).

$$\begin{aligned} k_{ov.}(T) &= \frac{k_{R1a}(T) \times k_{R1b}(T)}{k_{R\text{-}1a}(T) + k_{R1b}(T)} \\ &\cong \frac{k_{R1a}(T) \times k_{R1b}(T)}{k_{R\text{-}1a}(T)} \\ &= K_{R1a}(T) \times k_{R1b}(T) \end{aligned} \quad (2)$$

By invoking the canonical transition-state rate theory and statistical thermodynamics,[51–53] eqn (2) takes the following form

$$\begin{aligned} k_{ov.}(T) &= L\kappa \frac{k_B T}{h} \frac{(Q^{\ddagger}_{TS}/V)}{(Q_{Br}/V)(Q_{xylene}/V)} \\ &\quad \times \exp\left[-\frac{\{E_{TS} - (E_{Br} + E_{xylene})\}}{k_B T}\right] \end{aligned} \quad (3)$$

where $E_{TS} - [E_{Br} + E_{xylene}]$ is the net zero-point corrected energy barrier for the overall reaction. E_{TS}, E_{Br} and E_{xylene} are the total energy of the transition state, Br atom and xylene, respectively; Q denotes the molecular partition function of the species identified by the subscript; V is the volume; k_B is Boltzmann's constant; h is Planck's constant and L is the reaction path degeneracy. Partition functions were calculated using the rigid rotor-harmonic oscillator approximation except for the low-lying torsional modes (the vibrational wavenumbers corresponding to the torsional modes are shown in bold in Tables S1–S3 of ESI†). The torsional modes are treated either as free rotors or 1-D symmetrical hindered rotors. The electronic partition functions were set equal to the spin multiplicity *i.e.* 1 and 2 for the xylenes and TSs, respectively, whereas the electronic partition function of the Br atom was calculated using $Q_e(T) = 4 + 2\cdot\exp(-44\,085\ \text{J mol}^{-1}/RT)$ in which R is the universal gas constant. Due to the spin–orbit coupling, the two quantum states of the Br atom, $^2P_{3/2}$ and $^2P_{1/2}$, differ by an energy of 44.085 kJ mol^{-1} and have quantum weights of 4 and 2, respectively.[54] The reaction path degeneracy was calculated using $L = \frac{m_{TS} \times \sigma_{reactant}}{m_{reactant} \times \sigma_{TS}}$. Here, σ and m are the external symmetry numbers and number of optical isomers of the reactants and the transition states, respectively. For xylene + Br reactions, L equals 6 for the hydrogen abstraction reaction at the methyl site of the xylenes. κ is the transmission coefficient which takes into account the tunneling corrections. The effect of quantum tunneling on the calculated rate coefficients for the elementary step (pre-reactive complex → post-reaction complex) was calculated using Eckart tunneling through a 1-D unsymmetrical barrier. The temperature-dependent rate coefficients and equilibrium constants were computed using the THERMO tool of the MultiWell Master Equation Program Suite.[55]

Note that the pre-reactive complex (xylene···Br) does not appear in eqn (3). This may look as if the reaction is a single-step process and xylene···Br has no kinetic relevance. However, eqn (3) implicitly embodies the role of xylene···Br in the quantum tunneling factor (κ). As indicated earlier, the pre-reactive complex may play a critical role at low temperatures where quantum tunneling becomes important. As the quantum tunneling factor depends upon the height and curvature of the reactive potential energy surface, the exclusion of the addition complex in the kinetic analysis may cause underprediction of the tunneling corrections. Therefore, we used eqn (3) for the kinetic analyses to appropriately assess the tunneling correction.

3. Results and discussion

3.1 Diethyl ether (DEE) measured relative to toluene

As indicated in the Experimental section, we measured the rate coefficient for the reaction of Br with DEE relative to the reaction of Br with toluene. The results are summarized in Table 2 and the dependence of the rate coefficients on temperature is presented in Fig. 2. Also, Fig. 2 compares our new results with the results of our earlier measurement of these rate coefficients[24] and the results of the Kondo and Benson[56] obtained using the Very Low Pressure Reactor (VLPR) method. Conversion of Kondo and Benson[56] results to the format and units used elsewhere in the current work leads to $\log_{10}(k(\mathrm{cm^3\ molecule^{-1}\ s^{-1}})) = (-10.0 \pm 0.7) - (850 \pm 220)/T$. Our previous results[24] give $\log_{10}(k) = (-9.53 \pm 0.42) - (1060 \pm 140)/T$ with a linear correlation coefficient of 0.826. The results of the current measurements agree with our previous work within their combined standard deviations but it is clear from Fig. 2 that the agreement improves with increasing temperature. Both our current measurements and our earlier results are in satisfactory agreement with those of ref. 56, over the temperature range of our experiments, considering the large uncertainties reported for their Arrhenius coefficients. The current results fit the Arrhenius expression $\log_{10}(k) = (-7.69 \pm 0.55) - (1700 \pm 180)/T\ \mathrm{cm^3\ molecule^{-1}\ s^{-1}}$ with a linear correlation coefficient of 0.950. We have elected to use this expression to calculate the rate coefficients required when diethyl ether was used as the reference reactant. The basis for this decision is that the reaction of iso-octane with Br, used as the reference reaction in our earlier work, has a rate coefficient that is roughly a factor of ten smaller than the rate coefficient for the reaction of diethyl ether with Br. Moreover, the rate coefficient is approximately a factor of two smaller than that of the reaction of Br with toluene which we used as the reference reaction in the current work. As described in the Experimental section, this would have made it more difficult to obtain good analytical precision for the rate coefficient ratios measured in our earlier experiments. The correlation coefficient for the more recent results is also somewhat better than that for the earlier data. The Arrhenius pre-exponential factor has a large uncertainty as a result of the long extrapolation from the narrow temperature range accessible in our experiments. The average deviation of the rate coefficients from those calculated with the Arrhenius expression, over our range of experimental temperatures, is ±10% while the mean standard deviation of the slopes of the relative rate plots is ±13%. This suggests that the main contributor to the scatter of the rate coefficients is the chromatographic analysis required in the kinetic measurements.

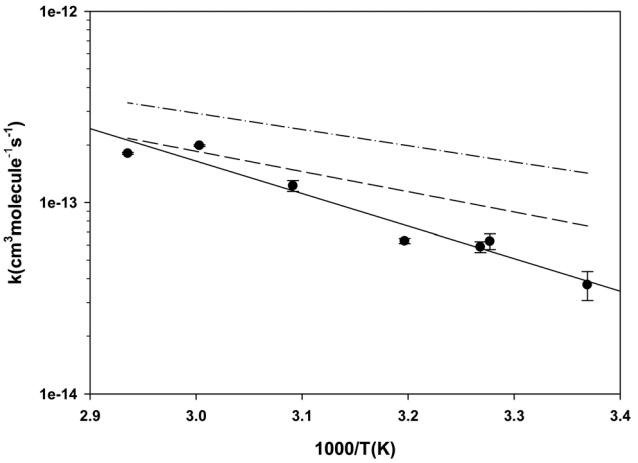

Fig. 2 Temperature dependence of the rate coefficients for the reaction of Br with diethyl ether. The filled circles represent the results of the current work in which toluene was the reference reactant. The dashed line is calculated from the results reported in ref. 24 in which the reference reactant was iso-octane. The dash-dot-dash line is calculated from the Arrhenius expression reported in ref. 56.

3.2 Reactions of Br with the xylenes

Our kinetic data for the reactions of the xylenes with Br are summarized in Tables 3 through 5 and in Fig. 3. Also shown in Fig. 3 as open diamonds are the values of the rate coefficients reported by Bierbach *et al.*[26] for the reactions of Br atoms with the xylenes. To the best of our knowledge, these are the only available room temperature literature data. Those for *o*- and *p*-xylenes are virtually superimposed and the value for *m*-xylene is somewhat smaller. The rate coefficients from the literature for all three xylenes are larger than those measured in our work by the same proportion and the separation of the rate coefficients for the *o*- and *p*-isomers from that for the *m*-isomer is very similar to the separation of those rate coefficients in our experiments. Our results in the vicinity of 300 K are well within the combined standard deviations of our measurements and

Table 2 Summary of kinetic data for the reaction of Br with diethyl ether (DEE) measured relative to the reaction of Br with toluene[a]

T (K)	$[\mathrm{DEE}] \times 10^{-15}$ (molecules cm^{-3})	$[\mathrm{Toluene}] \times 10^{-15}$ (molecules cm^{-3})	$[\mathrm{Br_2}] \times 10^{-15}$ (molecules cm^{-3})	$\frac{k_{\mathrm{DEE+Br}}}{k_{\mathrm{toluene+Br}}}$	$k_{\mathrm{DEE+BR}} \times 10^{14}$ (cm^3 molecule^{-1} s^{-1})
296.8	4.30	3.03	12.4	2.44 ± 0.42	3.72 ± 0.64
305.2	4.72	3.08	15.0	3.54 ± 0.33	6.27 ± 0.59
306.0	6.69	3.22	13.0	3.26 ± 0.21	5.86 ± 0.38
312.8	7.27	4.95	12.7	3.12 ± 0.93	6.30 ± 0.19
323.5	7.93	2.78	20.9	5.09 ± 0.34	12.2 ± 0.8
333.0	8.58	3.61	23.5	7.17 ± 0.65	19.9 ± 0.2
340.7	1.22	3.61	19.3	5.85 ± 0.65	18.1 ± 0.2

[a] The reference rate coefficient is given[23] in cm^3 molecule^{-1} s^{-1} by the Arrhenius expression $\log_{10}(k(T)) = (-11.43 \pm 0.20) - (707 \pm 65)/T$. The uncertainties in the table represent one standard deviation and do not include a contribution from the uncertainty in the reference rate coefficient.

Table 3 Summary of kinetic data for the reaction of Br with *o*-xylene[a]

T (K)	[Reference] $\times 10^{-15}$ (molecules cm^{-3})	[*o*-Xylene] $\times 10^{-15}$ (molecules cm^{-3})	[Br_2] $\times 10^{-16}$ (molecules cm^{-3})	$\frac{k_{o\text{-xylene+Br}}}{k_{ref}}$	$k_{o\text{-xylene+Br}} \times 10^{14}$ (cm^3 molecule^{-1} s^{-1})
Toluene reference					
293.0	0.503	2.43	0.970	6.19 ± 0.17	8.77 ± 0.24
295.9	0.922	2.61	0.973	4.97 ± 0.22	7.44 ± 0.33
296.4	0.653	4.20	1.32	4.42 ± 0.21	6.69 ± 0.32
296.6	0.582	2.40	1.04	3.46 ± 0.20	5.26 ± 0.30
297.2	0.703	5.18	1.24	4.55 ± 0.12	6.99 ± 0.18
323.6	1.50	4.29	0.849	4.97 ± 0.12	11.9 ± 0.3
324.5	2.34	4.45	0.947	4.92 ± 0.26	12.0 ± 0.6
346.3	2.19	4.40	1.07	5.49 ± 0.56	18.3 ± 1.9
Diethyl ether (DEE) reference					
290.4	1.62	2.06	1.42	2.13 ± 0.07	6.16 ± 0.32
299.9	2.60	2.45	0.929	1.96 ± 0.10	8.71 ± 0.29
323.6	1.77	2.48	1.42	1.29 ± 0.02	14.9 ± 0.1
325.0	1.81	3.94	0.947	1.51 ± 0.25	18.4 ± 0.3
346.3	2.18	4.14	1.33	0.80 ± 0.06	20.4 ± 0.2

[a] The reference rate coefficients are given in cm^3 molecule^{-1} s^{-1} for toluene[23] by the Arrhenius expression $\log_{10}(k(T)) = (-11.43 \pm 0.20) - (707 \pm 65)/T$ and for diethyl ether by the expression given in Section 3.1. The uncertainties in the table represent one standard deviation and do not include a contribution from the uncertainty in the reference rate coefficient.

those of ref. 26. (The absolute uncertainties in the vicinity of 300 K from Table 1 are, for this work, approximately $\pm 0.4 \times 10^{-14}$ cm^3 molecule^{-1} s^{-1} to $\pm 0.9 \times 10^{-14}$ cm^3 molecule^{-1} s^{-1} while for the results of ref. 26 the uncertainties are approximately $\pm 1 \times 10^{-14}$ cm^3 molecule^{-1} s^{-1} to $\pm 2 \times 10^{-14}$ cm^3 molecule^{-1} s^{-1}.) The results obtained in our work with diethyl ether as the reference reactant are statistically indistinguishable from those obtained with toluene as the reference reactant. This provides some confidence that these reference reactants had no appreciable effect on the mechanism of the reactions of Br with the xylenes. Our results as a function of temperature are represented by the following relations: *o*-xylene + Br, $\log_{10}(k(T)) = (-10.03 \pm 0.35) - (921 \pm 110)/T$; *m*-xylene + Br, $\log_{10}(k(T)) = (-10.78 \pm 0.09) - (787 \pm 92/T)$; *p*-xylene + Br, $\log_{10}(k(T)) = (-9.98 \pm 0.39) - (956 \pm 121)/T$. As noted above with measurement of the temperature dependence of the rate coefficient for the reaction of Br with diethyl ether, the large uncertainty in the Arrhenius pre-exponential factors is attributable to the long extrapolation from a narrow range of temperatures. The average deviation of the measured rate coefficients from those calculated from the Arrhenius expressions over our accessible temperature

Table 4 Summary of kinetic data for the reaction of Br with *m*-xylene[a]

T (K)	[Reference] $\times 10^{-15}$ (molecules cm^{-3})	[*m*-Xylene] $\times 10^{-15}$ (molecules cm^{-3})	[Br_2] $\times 10^{-16}$ (molecules cm^{-3})	$\frac{k_{m\text{-xylene+Br}}}{k_{ref}}$	$k_{m\text{-xylene+Br}} \times 10^{14}$ (cm^3 molecule^{-1} s^{-1})
Toluene reference					
292.2	1.02	2.15	1.13	2.59 ± 0.15	3.62 ± 0.21
298.0	0.732	5.13	1.02	3.28 ± 0.25	5.11 ± 0.39
299.6	0.851	4.06	1.46	2.43 ± 0.06	3.91 ± 0.10
300.7	0.907	3.75	1.92	2.46 ± 0.14	4.02 ± 0.23
303.5	2.47	7.39	2.26	2.76 ± 0.08	4.75 ± 0.14
303.7	3.10	6.73	2.03	2.70 ± 0.17	4.65 ± 0.29
303.7	3.70	8.04	2.37	2.49 ± 0.08	4.30 ± 0.14
303.8	1.93	7.62	1.74	2.53 ± 0.06	4.38 ± 0.10
313.2	2.35	6.89	2.15	2.43 ± 0.09	4.93 ± 0.12
324.0	2.63	7.38	2.09	2.62 ± 0.07	6.33 ± 0.17
332.8	2.68	6.83	1.76	2.85 ± 0.01	7.87 ± 0.03
340.7	3.44	7.78	1.72	2.70 ± 0.12	8.33 ± 0.37
Diethyl ether (DEE) reference					
294.8	4.01	7.22	2.41	0.82 ± 0.07	2.90 ± 0.25
295.7	5.68	7.33	2.28	0.93 ± 0.14	3.41 ± 0.51
304.2	1.75	9.67	1.86	0.65 ± 0.03	3.48 ± 0.16
312.5	4.11	6.91	2.15	0.51 ± 0.03	3.83 ± 0.23
323.5	4.64	5.14	1.87	0.42 ± 0.05	4.84 ± 0.58
333.2	4.97	5.03	2.37	0.45 ± 0.05	7.35 ± 0.82
340.7	5.00	5.92	1.82	0.41 ± 0.04	8.60 ± 0.84

[a] The reference rate coefficients are given in cm^3 molecule^{-1} s^{-1} for toluene[23] by the Arrhenius expression $\log_{10}(k(T)) = (-11.43 \pm 0.20) - (707 \pm 65)/T$ and for diethyl ether by the expression given in Section 3.1. The uncertainties in the table represent one standard deviation and do not include a contribution from the uncertainty in the reference rate coefficient.

Table 5 Summary of kinetic data for the reaction of Br with *p*-xylene[a]

T (K)	[Reference] $\times 10^{-15}$ (molecules cm^{-3})	[*p*-Xylene] $\times 10^{-15}$ (molecules cm^{-3})	[Br_2] $\times 10^{-16}$ (molecules cm^{-3})	$\frac{k_{p\text{-xylene+Br}}}{k_{ref}}$	$k_{p\text{-xylene+Br}} \times 10^{14}$ (cm^3 molecule^{-1} s^{-1})
Toluene reference					
295.0	2.51	5.70	1.25	2.61 ± 0.25	3.85 ± 0.37
303.7	2.42	6.79	2.38	4.28 ± 0.14	7.38 ± 0.24
304.0	2.36	7.68	2.03	4.24 ± 0.14	7.36 ± 0.24
305.3	2.10	1.93	0.922	4.45 ± 0.31	7.91 ± 0.55
313.2	2.49	7.21	1.27	5.34 ± 0.10	10.8 ± 0.2
323.7	1.67	2.68	1.22	5.07 ± 0.25	12.2 ± 0.6
332.7	1.59	6.54	1.81	4.48 ± 0.21	12.3 ± 0.6
340.5	2.04	6.65	2.44	5.05 ± 0.17	15.6 ± 0.5
Diethyl ether (DEE) reference					
295.2	1.70	6.82	1.45	1.79 ± 0.13	6.46 ± 0.47
295.3	2.19	7.90	1.14	1.90 ± 0.09	6.89 ± 0.33
306.7	1.63	6.21	1.70	1.52 ± 0.10	9.01 ± 0.59
312.8	1.82	6.29	1.37	1.25 ± 0.10	9.48 ± 0.76
323.5	1.64	6.16	2.20	0.99 ± 0.06	11.3 ± 0.7
333.3	1.87	7.03	2.03	0.83 ± 0.07	13.6 ± 1.1

[a] The reference rate coefficients are given in cm^3 molecule^{-1} s^{-1} for toluene[23] by the Arrhenius expression $\log_{10}(k(T)) = (-11.43 \pm 0.20) - (707 \pm 65)/T$ and for diethyl ether by the expression given in Section 3.1. The uncertainties in the table represent one standard deviation and do not include a contribution from the uncertainty in the reference rate coefficient.

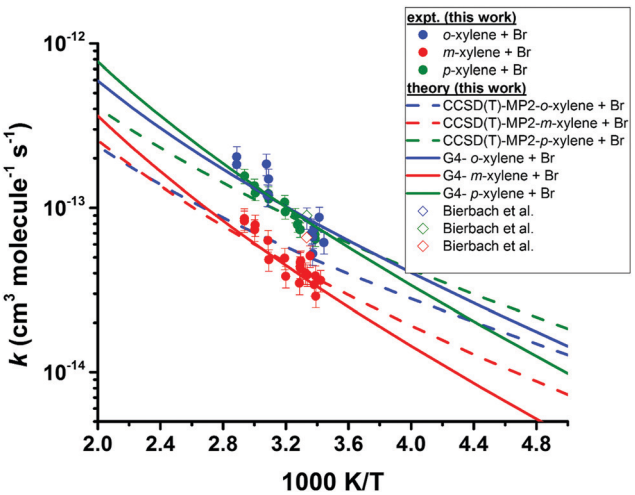

Fig. 3 Temperature dependence of the rate coefficients for the reactions of Br with the xylenes. The filled circles represent the experimental results from this work. The open diamonds represent the results of Bierbach *et al.*[26] obtained at 300 ± 2 K in 1000 millibar of synthetic air (1 bar = 10^5 Pa). The lines represent the theoretical rate coefficients obtained after lowering the barrier height of the corresponding transition states by ≤1.5 kJ mol^{-1} at both the indicated levels of theory (see text for explanation).

range was about ±10% and this was of similar magnitude to the average relative deviation in the measurements of the slopes of the relative rate plots.

The measured rate coefficients for the reaction of Br with toluene and for the reactions of Br with the xylenes showed notable temperature dependence indicating a sizable activation barrier for the corresponding reaction. The measurable activation energies display some selectivity to the organic reactant. However, within the experimental uncertainty, we consider the activation energies of these four reactions to be identical. The rate coefficients for the reactions of *o*- and *p*-xylene with Br are statistically indistinguishable over the temperature range of our experiments. At 300 K, the reaction of Br with *m*-xylene is approximately a factor two slower than the reactions of Br with *o*- and *p*-xylene at the same temperature. The rate coefficient for the reaction of Br with toluene is approximately 25% of the values for the corresponding reactions of *o*- and *p*-xylenes at the same temperature. This is similar to the results reported in ref. 26. At 300 K, our measured values of the rate coefficients for the Br atom reactions with toluene and the xylenes show a nice agreement with those of Bierbach *et al.*[26] (see Table 1 and Fig. 3).

3.3 Potential energy surface, thermochemistry and rate coefficients

Ring hydrogen abstraction and substitution reactions. The reactions of Br atoms with the xylenes offer various reaction pathways on the potential energy surfaces (PES). The pathways may include abstraction, addition and substitution reactions. The abstraction of a hydrogen atom by a Br atom may take place either from a sp^2 C–H bond (ring hydrogen) or a sp^3 C–H bond (methyl hydrogen). In a previous kinetic study, Bierbach *et al.*[26] observed no detectable decay of benzene in the benzene + Br reaction. This allowed the authors to estimate the upper limit of the rate coefficients ($k_{benzene+Br} \leq 5 \times 10^{-16}$ cm^3 molecule^{-1} s^{-1}). In our companion study for the toluene + Br reaction,[9] we found that ring hydrogen abstraction is highly endothermic [$\Delta_{rxn,0K}H^\circ$ = (107.1 ± 3.4) kJ mol^{-1}] (see Fig. S1 of ESI†). We were able to locate the corresponding transition state, which lies ∼115 kJ mol^{-1} higher than the reactants (toluene + Br) at the G3 level of theory. The calculated rate coefficient (∼10^{-24} cm^3 molecule^{-1} s^{-1} at 500 K) for abstraction of the ring hydrogen of toluene by Br atoms was too small to measure. This shows that Br atoms are unreactive with benzene. This finding is in line with the experimental observation of Bierbach *et al.*[26] For a given *ab initio* method, the standard enthalpy of reaction ($\Delta_{rxn,0K}H^\circ$) for ring hydrogen abstraction is very comparable to the Br atom reactions

Table 6 Calculated standard enthalpy of reaction at 0 K ($\Delta_{rxn,0K}H^{\circ}$) for xylenes + Br reaction system at various levels of theory

	$\Delta_{rxn,0K}H^{\circ}$ (kJ mol^{-1})			
Reaction	G3	G4	CCSD(T)/cc-pV(D,T)Z//MP2/aug-cc-pVDZ	CCSD(T)/cc-pV(D,T)Z//B3LYP/cc-pVTZ
m-Xylene + Br → 3-methyl benzyl + HBr	10.5	9.1	4.4	1.3
m-Xylene + Br → 3,5-dimethyl phenyl + HBr	109.8	101.8	104.3	95.5
m-Xylene + Br → 2,4-dimethyl phenyl + HBr	112.0	104.2	106.0	97.9
m-Xylene + Br → 2,6-dimethyl phenyl + HBr	110.2	101.8	103.7	95.8
o-Xylene + Br → 2-methyl benzyl + HBr	10.4	9.3	4.4	0.4
o-xylene + Br → 3,4-dimethyl phenyl + HBr	112.2	103.9	106.3	96.8
o-Xylene + Br → 2,3-dimethyl phenyl + HBr	110.0	101.2	104.7	94.9
p-Xylene + Br → 4-methyl benzyl + HBr	10.1	8.7	3.9	−0.3
p-Xylene + Br → 2,5-dimethyl phenyl + HBr	110.2	102.0	104.3	94.7

with toluene and the xylenes (*cf.* Table 6 and Fig. S1 of ESI†). Hence, we conclude that the abstraction of ring hydrogen atoms by Br atoms from aromatics is kinetically irrelevant.

None of the *ab initio* methods employed here for geometry optimizations could locate the transition states corresponding to the ring hydrogen abstraction. Note that G3 utilizes the HF/6-31G(d) level of theory for geometry optimization and frequency calculations, then employs the MP2(full)/6-31G(d) level of theory to reoptimize the structure before embarking on the single point calculations, whereas G4 utilizes the B3LYP/6-31G(2df,p) level of theory for the same purpose. We further utilized the MP2/aug-cc-pVDZ and B3LYP/cc-pVTZ levels of theory for geometry optimizations and frequency calculations. The convergence for the geometry optimization failed at both the MP2 and B3LYP levels of theory for all the basis sets studied here. Therefore, we conclude that the abstraction of aromatic ring hydrogen atoms by a Br atom takes place seemingly *via* a loose transition state where the new H···Br bond formation and C···H bond breaking may be occurring simultaneously (SN2 type of reaction). A similar conclusion was made by Ryzhkov *et al.*[25] where the authors could not locate the transition state for the ring hydrogen abstraction from benzene and toluene by Cl atoms. Whether the ring hydrogen abstraction occurs *via* a tight or loose transition state, these reactions are very energy demanding ($\Delta_{rxn,0K}H^{\circ} > 102$ kJ mol^{-1}). Therefore, they seem highly unlikely to compete with the hydrogen abstraction reaction from the methyl site of the xylenes. Besides, the reaction pathways for the substitution of a ring hydrogen atom or methyl group of the xylenes by a Br atom are also kinetically irrelevant. Such a conclusion may be justified when the xylene + Br reaction systems are taken in analogy with the toluene + Br reaction system (see our recent work[9] and Table S7 (ESI†) for the reaction enthapies of such chemical processes). Therefore, we expect that the substitution reactions for xylene + Br sytems are energetically too high and can safely be ruled out in the same way as that in the toluene + Br reaction system.

Methyl hydrogen abstraction. In light of the above discussion, the only plausible reaction for xylenes + Br appears to be the hydrogen abstraction from the methyl group of the xylenes by a Br atom *via* the reaction sequence (R1a)–(R1c). As seen in Fig. 4, the reaction proceeds in a three-step process *via* an addition–elimination mechanism in an overall endothermic process. The reaction complexes appear both at the entrance and exit channels.

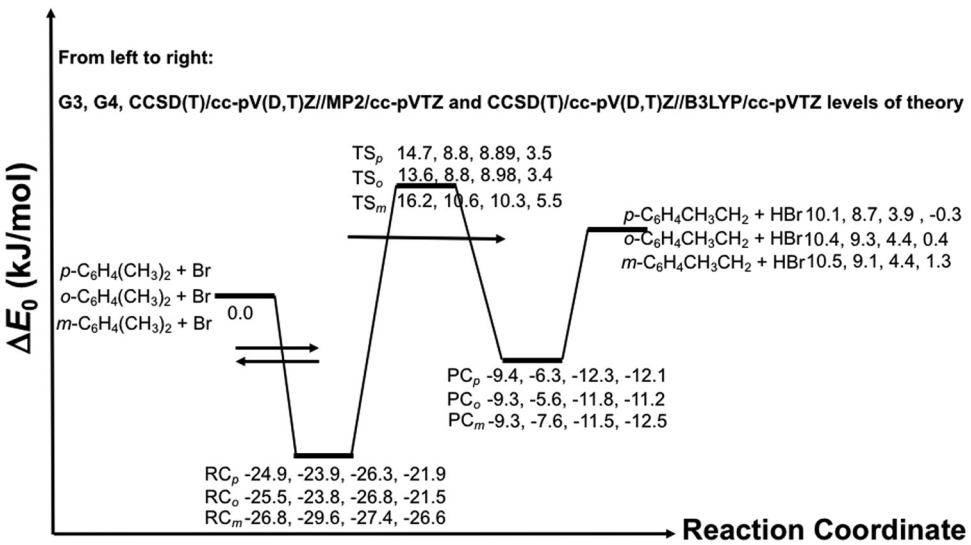

Fig. 4 Zero-point energy corrected potential energy surface for the reaction of Br atoms with the xylenes. RC, TS and PC stand for pre-reactive complex, transition state and post-reactive complex, whereas the subscripts identify the species of the xylene isomer being considered (*e.g.* TS_o identifies the transition state corresponding to the *o*-xylene + Br reaction). The arrows indicate a pre-equilibrium kinetics scenario.

At the entrance channel, the attractive interaction between the xylene and a Br-atom results in the formation of a pre-reactive complex (RH···Br═RC) which lowers the energy of the isolated reactants by >22 kJ mol^{-1}. Several complexes are possible by the interaction of a Br atom with the xylenes. However, the kinetically relevant RC is a π-complex, which is characterized by a weak three-center bond between the Br-atom and two carbon atoms of the aromatic ring at the vicinity of the $-CH_3$ group. The shorter bond length between the carbon and Br atom measures *ca.* 2.7 Å in each case (see the optimized structures of the complexes in Fig. S2 of ESI†). Note that, while forming the pre-reactive complex, the rest of the molecule is barely perturbed by the interaction.

Here, the RC is energetically at least 4 kJ mol^{-1} more stable than that of the toluene + Br system (*cf.* Fig. 4 and Fig. S1 of ESI†). This extra stabilization energy of the RC can be attributed to the electron-donating character of the two methyl groups in the xylenes as opposed to one methyl group in toluene. Additionally, the relative stability of the RCs in the xylenes + Br reaction systems are found to be in the same order as that seen in the reactions of Cl, Br and OH with oxygenated VOCs *e.g.* 1,4-dioxane,[8,11] tetrahydropyran,[7] tetrahydrofuran,[10,14] methanol,[12,15,16,57] ethyl propyl ether[57] *etc.* A new feature that appears in reactions of OH with oxygenated VOCs is the possibility of hydrogen bonding in the structures of the intermediate complexes and transition states. A very recent study[24] on the reaction of OH with ethyl propyl ether reports the relative stability of the pre-reactive complexes in the range -24.4 to -26.6 kJ mol^{-1} which is very similar to the exothermicity of the corresponding processes for the reactions of Cl and Br with the oxygenated VOCs.

Formation of the post-reactive complexes (R···HX═PC) in the reactions of OH with oxygenated VOCs is highly exothermic in comparison. The stabilities of the post-reactive complexes lie in the range -81.7 to -117.4 kJ mol^{-1}, whereas the standard enthalpies of reaction ($\Delta_{rxn,0K}H^\circ$) of the reaction products range from -72.1 to -103.3 kJ mol^{-1}.[13,14,57] This is not surprising considering the fact that any water forming reactions in hydrocarbon systems are always highly exothermic. On the contrary, the reactions of Br atoms with VOCs are endothermic processes. Accordingly, the relative positions of the post-reactive complexes and the transition states vary from one chemical system to the other. As a consequence of the complex forming mechanism, the oxygenated VOCs display a wide but interesting variation in reaction kinetics with important atmospheric radical species like OH, Cl and Br. At low temperatures, the importance of the degree of stabilization of the pre-reactive complex for accurate description of the pressure dependence of the reaction of OH radicals with CH_3OH has been highlighted recently by Gao *et al.*[16] and Shannon *et al.*[15] In these studies, the authors were able to nicely describe the unusually high rate coefficients for the reaction of OH radicals with CH_3OH at ultracold temperatures by employing theoretical methods. The importance of OH bound complexes in the bimolecular reactions of the OH radical has been reviewed recently.[58,59] This highlights the importance of the weakly bound complexes to accurately describe the kinetic picture of several complex forming reactions.

As seen in Fig. 4, the exothermicity of formation of the pre-reactive complex (RC) shows a strong dependence on the level of theory used. Therefore, it is often risky to rely on a single method, particularly if the method fails unexpectedly in characterizing the electronic structure of a given species. Here, we have first employed the G3 and G4 composite methods to characterize the reactions of Br atoms with the xylenes. CBS-QB3 is not an appropriate method for the current system as it is known to give highly erroneous results, particularly for systems containing aromatic radicals.[9] The CBS-QB3 based enthalpy of formation of the phenyl radical has a large deviation of 19.43 kJ mol^{-1} from the accurate ATcT data base.[60] We have demonstrated the inappropriateness of the CBS-QB3 method in our companion study[9] for the toluene + Br reaction. As stated earlier, other popular composite methods like CBS-APNO and W1U cannot be applied for Br containing chemical systems. For a given xylene + Br system, the G3 and G4 methods predict similar relative stability of the corresponding RC. The G3 and G4 values for the relative stability of the RC are reinforced by the CCSD(T)/cc-pV(D,T)Z//MP2/aug-cc-pVDZ and CCSD(T)/cc-pV(D,T)Z//B3LYP/cc-pVTZ levels of theory. The stabilization energies of a given RC from various *ab initio* methods match within chemical accuracy ($\sim$4.2 kJ mol^{-1}). As discussed earlier, the relative position of the RC on the PES does not alter the overall kinetics as long as quantum tunneling is not important. Here, the most crucial part is the relative position of the transition state as its location dictates the accuracy of the predicted value of the rate coefficient. Unfortunately, the barrier heights (ΔE_0) are found to be sensitive to the quantum method used. For example, among the *ab initio* methods employed, the CCSD(T)/cc-pV(D,T)Z//B3LYP/cc-pVTZ level of theory predicts the lowest barrier height, whereas the barrier height with the G3 composite method is the highest for a given xylene + Br reaction. The predicted barrier heights from these two methods differ by at least 10 kJ mol^{-1}. We observed a similar trend for the toluene + Br reaction.[9] This warrants a closer look into the individual methods in terms of chemical accuracy.

The choice of an appropriate *ab initio* method. As seen in Fig. 4, the relative positions of the stationary points on the PES of the xylenes + Br reactions highly depend upon the *ab initio* methods used. Even the overall enthalpy of reaction shows a difference as large as 10 kJ mol^{-1}. To assess the source of this discrepancy, we begin by checking the extent of spin contamination in the unrestricted version of the *ab initio* methods used here. For a doublet species, the expected value of the spin $\langle S^2 \rangle$ should equal 0.75 if there is no contamination from the higher spin states. If the spin contamination is large, the potential energy surface predicted by the unrestricted wave functions can be significantly distorted which may lead to poor reference geometry, anomalous vibrational frequencies and high reaction barriers.[61] A closer look revealed that G3 suffers from large spin contamination *e.g.* $\langle S^2 \rangle$ = 1.008 and 1.028 even after the spin annihilation step for TS_p and p-$C_6H_4CH_3CH_2$, respectively. We noted earlier that G3 reoptimizes geometry at the MP2(full)/

6-31G(d) level of theory. Consequently, we expect that the MP2/aug-cc-pVDZ level of theory will also suffer from severe contamination by the higher spin states. Indeed, $\langle S^2 \rangle$ after spin annihilation was found to be 1.039 and 1.033 for TS_p and p-$C_6H_4CH_3CH_2$, respectively. Therefore, the optimized geometry at the MP2 level of theory may yield inaccurate thermochemical properties and kinetics for the reactions of Br atoms with the xylenes. Considering that G4 utilizes B3LYP/6-31G(2df,p), a hybrid density functional theory (DFT) with 20% HF exchange, for geometry optimization before embarking into several single-point energy calculations, this composite method can be effective in eliminating spin contamination. It is known that the DFT densities and energies are less affected by spin contamination than the corresponding unrestricted Hartee–Fock quantities.[62–64] The $\langle S^2 \rangle$ values were found to be 0.75034 and 0.7507 for TS_p and p-$C_6H_4CH_3CH_2$, respectively, revealing that the G4 method shows negligible spin contamination as expected. Similar to our earlier work on the toluene + Br system,[9] the G4 parameters captured the experimental kinetic data satisfactorily. Likewise, the G4 parameters yielded accurate thermochemical properties such as enthalpy of reaction and enthalpy of formation (see subsequent discussion). Although the MP2 geometries may be affected by spin contamination, the barrier heights calculated at the CCSD(T)/cc-pV(D,T)Z//MP2/aug-cc-pVDZ level of theory perfectly match those from the G4 method. Note that the CCSD(T) method has been found to be relatively insensitive to the choice of restricted or unrestricted calculations.[65,66] That being said, the difference in the predicted energies calculated with the restricted (ROHF-CCSD(T)) or unrestricted (UHF-CCSD(T)) procedures is negligibly small.

The barrier heights at the G3 level of theory are too high which may result from the severe spin contamination, whereas they are too low at the CCSD(T)/cc-pV(D,T)Z//B3LYP/cc-pVTZ level of theory. In addition, the reaction enthalpy predicted at the CCSD(T)/cc-pV(D,T)Z//B3LYP/cc-pVTZ level of theory is almost thermoneutral which seems highly unlikely. This suggests that the G4 method outperforms all the levels of theory used here (see also the discussion below).

Comparing the geometrical parameters obtained at the MP2/aug-cc-pVDZ and B3LYP/6-31G(2df,p) levels of theory may help to assess the method dependence of the transition-state structures. Fig. 5 depicts the equilibrium geometrical parameters for the transition states obtained at the MP2/aug-cc-pVDZ and B3LYP/6-31G(2df,p) levels of theory. As can be seen, the optimized geometry differs significantly for a given transition state. For instance, MP2/aug-cc-pVDZ predicts the breaking of C···H at a bond length of ~1.45 Å, whereas it is further stretched to at least 1.59 Å at the B3LYP/6-31G(2df,p) level of theory. Furthermore, the incoming Br atom is found to be somewhat farther apart from the hydrogen atom being abstracted at the MP2/aug-cc-pVDZ level of theory. The length of the forming H···Br bond is 1.58 Å and 1.55 Å at the MP2/aug-cc-pVDZ and B3LYP/6-31G(2df,p) levels of theory, respectively. Therefore, the MP2 optimized TS structure reveals an early transition state as opposed to the B3LYP structure. In fact, at both levels of theory, the predicted TS structure has a character more like that of the products as the breaking C···H bond is far

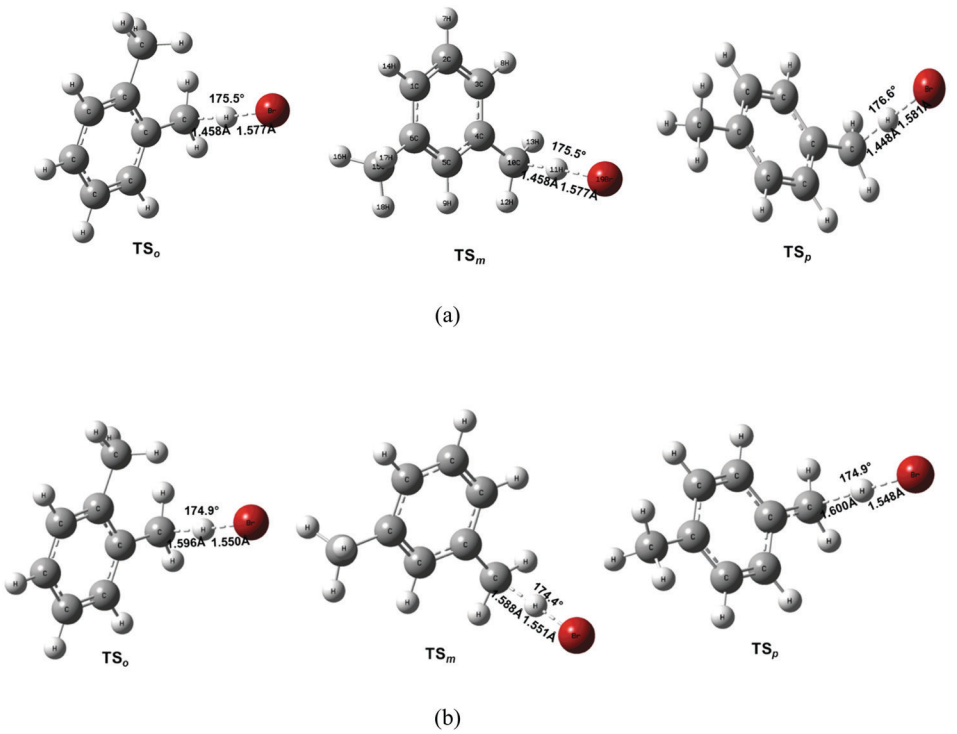

Fig. 5 Geometric parameters of the transition states optimized at (a) MP2/aug-cc-pVDZ and (b) B3LYP/6-31G(2df,p) levels of theory. The optimized structures of pre-reactive and post-reactive complexes are provided in Fig. S2 of ESI.†

too stretched from the normal C–H (1.09 Å in toluene) and the forming H···Br bond distance is already close to the normal H–Br bond length (the lowest value being 1.43 Å). In all cases, the attack of the Br atom on the H–C bond is nearly collinear *i.e.* the bond angle, δ(C···H···Br), is close to 175°. Another notable difference between the MP2 and B3LYP optimized parameters is the imaginary frequency. The imaginary frequency, which characterizes the nature of the transition state, shows a large difference. MP2 imaginary frequencies are quite large as compared to those from the B3LYP level of theory (see Tables S1–S3, ESI†). Note that a large imaginary frequency indicates a tight transition state with a large curvature making quantum tunneling more important.[9]

Thermochemistry. Table 7 lists the calculated values of the standard enthalpies of formation of the xylenes and their radicals using atomization schemes of various model chemistries and their combinations. In terms of accuracy, Somers and Simmie[60] report that the combination of G4/CBS-APNO methods outperforms all the individual methods. If other methods are available, the authors recommend use of the combination of CBS-APNO/G4/G3 as this combination yields the most reliable average value for the standard enthalpy of formation of closed shell and radical species. Interestingly, CBS-APNO values for the standard enthalpies of formation of the xylenes show large deviations (lower by ~15 kJ mol^{-1}) compared to the G3 and G4 values. We made a similar observation for toluene as well [$\Delta_{f,0K}H^\circ$ = 61.1 kJ mol^{-1} from CBS-APNO *vs.* 73.29 kJ mol^{-1} from the Active Thermochemical Tables (ATcT)[48]]. On the other hand, we found that G3 ($\Delta_{f,0K}H^\circ$ = 75.1 kJ mol^{-1}) and G4 ($\Delta_{f,0K}H^\circ$ = 73.7 kJ mol^{-1}) values for enthalpy of formation of toluene agree excellently with the ATcT database. We chose to benchmark against the ATcT database because it lists the most reliable internally consistent set of thermochemical properties which sets a new standard of accuracy in thermochemistry by systematically lowering the thermochemical uncertainties. Unfortunately, the ATcT thermodynamic database values are still not available for the xylenes and their corresponding radicals. Therefore, we compare our data with the available literature data wherever possible. The G3 and G4 values for the standard enthalpies of formation of the xylenes are close to each other and agree excellently with those from Prosen *et al.*[67] and the isodesmic scheme (see Table 7) whereas the CBS-APNO values are too low. Therefore, the CBS-APNO values for the enthalpies of formation of xylenes are not included for averaging. Nonethless, for open shell species, the CBS-APNO values for the enthalpy of formation are not far off from the G4 and G3 values. Therefore, CBS-APNO values are still included for averaging of the enthalpies of formation of the radicals derived from the xylenes.

As seen in Table 7, the G4/CBS-APNO duo approach gives a standard deviation of ~1 kJ mol^{-1} and ~2 kJ mol^{-1} for $\Delta_{f,298K}H^\circ$ and $\Delta_{f,0K}H^\circ$ of ring-carbon centered radicals, respectively. As for the benzyl type radicals, the standard deviation is as large as ~7 kJ mol^{-1}. The standard enthalpies of formation of the radicals obtained at the G3 level of theory are systematically higher than those of the other two composite methods. Therefore, inclusion of G3 data yields higher values for the formation enthalpy of the species with standard deviations as large as 7.5 kJ mol^{-1}. Consequently, isodesmic reaction schemes were applied to check the accuracy of the predicted enthalpy of formation of the radical species. The standard enthalpies of formation of benzyl type radicals were calculated using a hypothetical reaction, $C_6H_5CH_3$ ($\Delta_{f,0K}H^\circ$ = 73.29 kJ mol^{-1}) + $^\bullet CH_2$–CH=CH_2

Table 7 Computed standard enthalpies of formation for the xylenes and their radicals at 0 K ($\Delta_{f,0K}H^\circ$) and 298.15 K ($\Delta_{f,298K}H^\circ$) using atomization schemes of various model chemistries. Δ_fH° is given in units of kJ mol^{-1}

	CBS-APNO		G4		G3		CBS-APNO/G4 ($\pm1\sigma$)		CBS-APNO/G4/G3($\pm1\sigma$)	
	$\Delta_{f,0K}H^\circ$	$\Delta_{f,298.15K}H^\circ$	$\Delta_{f,0K}H^\circ$	$\Delta_{f,298.15K}H^\circ$	$\Delta_{f,0K}H^\circ$	$\Delta_{f,298.15K}H^\circ$	$\Delta_{f,0K}H^\circ$	$\Delta_{f,298.15K}H^\circ$	$\Delta_{f,0K}H^\circ$	$\Delta_{f,298.15K}H^\circ$
m-Xylene	30.3	6.1	45.3	18.6	46.5	20.05	45.3[a]	18.6[a]	45.9(0.8)[a] 46.1[b]	19.3(1.1)[a] 17.2 ± 0.8[c]
3,5-Dimethyl phenyl	291.2	271.7	291.3	268.8	302.8	281.3	291.3(0.1)	270.2(2.1)	295.1(6.7)	273.9(6.5)
2,4-Dimethyl phenyl	292.7	273.2	293.6	270.9	305.0	283.4	293.2(0.6)	272.0(1.6)	297.1(6.9)	275.8(6.6)
2,6-Dimethyl phenyl	291.3	271.9	291.2	268.8	303.2	281.6	291.3(0.1)	270.3(2.2)	295.2(6.9)	274.1(6.7)
3-Methyl benzyl	190.3	169.4	198.6	174.5	203.4	180.5	194.5(5.9)	171.9(3.6)	197.4(6.6) 199.3[b]	174.8(5.5)
o-Xylene	29.6	4.1	46.0	17.9	47.2	19.4	46.0[a]	17.9[a]	46.6(0.8)[a] 46.8[b]	18.7(1.1)[a] 18.9 ± 1.1[c]
3,4-Dimethyl phenyl	293.1	272.4	294	270.1	305.9	283.0	293.6(0.6)	271.2(1.6)	297.7(7.1)	275.1(6.9)
2,3-Dimethyl phenyl	289.9	269.4	291.8	268.0	303.8	281.0	290.9(1.3)	268.7(1.0)	295.2(7.5)	272.8(7.1)
2-Methyl benzyl	190.0	168.4	199.4	174.6	204.1	180.4	194.7(6.6)	171.5(4.4)	197.8(7.2) 200.2[b]	174.5(6.0)
p-Xylene	30.2	6	45.9	19.2	47.0	20.6	45.9[a]	19.2[a]	46.5(0.8)[a] 46.8[b]	19.9(1.0)[a] 17.9 ± 1.0[c]
4-Methyl benzyl	189.9	169.2	198.8	174.8	203.7	180.9	194.4(6.3)	172.0(4.0)	197.5(7.0) 199.5[b]	175.0(5.9)
2,5-Dimethyl phenyl	290.9	271.5	292.1	269.6	303.4	282.1	291.5(0.8)	270.5(1.4)	295.5(6.9)	274.4(6.8)

[a] Enthalpies of formation (Δ_fH°) values excluding the CBS-APNO method (see text for explanation). [b] Enthalpies of formation values of using the isodesmic reaction: for xylenes, 2 toluene ($\Delta_{f,0K}H^\circ$ = 73.29 kJ mol^{-1}) → *p*-, *o*-, *m*-xylene + benzene ($\Delta_{f,0K}H^\circ$ = 100.61 kJ mol^{-1}) and for benzyl type radicals, $C_6H_5CH_3$ ($\Delta_{f,0K}H^\circ$ = 73.29 kJ mol^{-1}) + $^\bullet CH_2$–CH=CH_2 ($\Delta_{f,0K}H^\circ$ = 180.03 kJ mol^{-1}) → *p*-, *o*-, *m*-$C_6H_5CH_3{\cdot}CH_2$ + CH_2=CH_2 ($\Delta_{f,0K}H^\circ$ = 60.88 kJ mol^{-1}) were considered. Here, the given enthalpies of formation were taken from the Active Thermochemical Tables (ATcT) and reaction enthalpy ($\Delta_{rnx,0K}H^\circ$) from zero-point corrected electronic energies of G4 calculations. [c] Enthalpy of formation values ($\Delta_{f,298K}H^\circ$) taken from Prosen *et al.*[67]

($\Delta_{f,0K}H^\circ$ = 180.03 kJ mol^{-1}) → *p*-, *o*-, *m*-$C_6H_5CH_3{\cdot}CH_2$ + $CH_2{=}CH_2$ ($\Delta_{f,0K}H^\circ$ = 60.88 kJ mol^{-1}). Here, the given formation enthalpies were taken from the ATcT database. By utilizing the enthalpies of reaction obtained from the zero-point corrected electronic energies of G4 calculations, the enthalpies of formation of *o*-$C_6H_5CH_3{\cdot}CH_2$, *m*-$C_6H_5CH_3{\cdot}CH_2$ and *p*-$C_6H_5CH_3{\cdot}CH_2$ at 0 K were calculated to be 200.2, 199.3 and 199.5 kJ mol^{-1}, respectively. These values are nearly identical to those predicted by the combination of the trio of G4/CBS-APNO/G3 methods. In addition, the G3 and G4 reaction endothermicities for a given $C_6H_5(CH_3)_2$ + Br reaction are very similar. This implies that the earlier notion of spin contamination affecting G3 parameters is not too severe, and hence we can hardly justify the exclusion of the G3 data for the evaluation of the thermochemical quantities. For these reasons, we conclude that there is no need to exclude CBS-APNO and G3 values for the enthalpy of formation of the xylene derived radical species.

For several reasons, we find that the G4 composite method performs the best among the *ab initio* methods used here for the xylene + Br chemical system: (i) the G4 parameters with a subtle adjustment of the barrier height reproduced the trend of the experimental kinetic data very well (see the subsequent section below). (ii) Using an atomization scheme, G4 data yielded $\Delta_{f,298K}H^\circ$[*o*-$C_6H_4(CH_3)_2$] = 17.9 kJ mol^{-1}, $\Delta_{f,298K}H^\circ$[*m*-$C_6H_4(CH_3)_2$] = 18.6 kJ mol^{-1} and $\Delta_{f,298K}H^\circ$[*p*-$C_6H_4(CH_3)_2$] = 19.2 kJ mol^{-1} which compared excellently with the experimental data of Prosen *et al.*[67] ($\Delta_{f,298K}H^\circ$[*o*-$C_6H_4(CH_3)_2$] = 18.9 ± 1.0 kJ mol^{-1}, $\Delta_{f,298K}H^\circ$[*m*-$C_6H_4(CH_3)_2$] = 17.2 ± 0.8 kJ mol^{-1} and $\Delta_{f,298K}H^\circ$[*p*-$C_6H_4(CH_3)_2$] = 17.9 ± 1.0 kJ mol^{-1}) (see Table 7). In addition, G4 enthalpy of formation values agree remarkably with the Burcat thermochemical database[49] *e.g.* $\Delta_{f,298K}H^\circ$[*o*-$C_6H_4(CH_3)_2$] = 18.5 kJ mol^{-1}, and $\Delta_{f,298K}H^\circ$[*p*-$C_6H_4(CH_3)_2$] = 19.6 kJ mol^{-1}. We made a similar observation for toluene and the benzyl radical. The G4 enthalpy of formation at 0 K using the atomization scheme yields $\Delta_{f,0K}H^\circ$ = 73.7 kJ mol^{-1} and 228.8 kJ mol^{-1} for toluene and the benzyl radical, respectively. These values match excellently with those listed in the ATcT database[48] [$\Delta_{f,0K}H^\circ$ ($C_6H_5CH_3$) = 73.29 ± 0.34 kJ mol^{-1} and $\Delta_{f,0K}H^\circ$ ($C_6H_5CH_2$) = 229.9 ± 0.6 kJ mol^{-1}]. Again, we note that the ATcT database[48] is currently the state-of-the-art thermochemical database. (iii) Similarly, in our earlier work,[9] G4 yielded a value of $\Delta_{rxn,0K}H^\circ$ = 10.9 kJ mol^{-1} for the enthalpy of reaction at 0 K of $C_5H_5CH_3$ + Br → $C_6H_5CH_2$ + HBr which shows very good agreement with the ATcT database ($\Delta_{rxn,0K}H^\circ$ = 10.75 ± 0.53 kJ mol^{-1}). Unfortunately, the ATcT thermodynamic database does not include the parameters for the xylenes and their corresponding radicals. However, for the xylenes + Br reactions, the enthalpy of reaction ($\Delta_{rxn,0K}H^\circ$) obtained from the G4 level of theory closely matches with that obtained from the enthalpy of formation values of the reacting species using the ATcT database and isodesmic values where ATcT values are not available.

Rate coefficients *k*(*T*). Our preceding discussion allows us to conclude that the reactions of Br atoms with the xylenes can only occur at the methyl site. The reaction proceeds by the interaction of a Br atom with the xylenes forming a pre-reactive complex which undergoes subsequent intramolecular rearrangement to form a post-reactive complex before eliminating HBr in an overall endothermic process. The reaction sequence (R1a)–(R1c) summarizes the overall process which is depicted in Fig. 4. The transition state linking the pre- and post-reactive complexes represents the highest point along the path of the reaction sequence (R1a)–(R1c). Hence, the transition state dictates the kinetics of the xylenes + Br reaction system. The formation of the pre-reactive complex is a barrierless process whose rate coefficient (k_{R1a}) is expected to be near the collision limit (k_{R1a} ~ 10^{-10} cm^3 molecule^{-1} s^{-1}). Since reaction (R1b) has a significantly higher barrier than the reverse reaction of (R1a), back dissociation of the pre-reactive complex to the reactants, (R-1a), is a much favored channel. Due to the much higher entropy of the loose transition state, reaction (R-1a) occurs much faster than (R1b). This can be readily seen when one combines k_{R1a} ~ 10^{-10} cm^3 molecule^{-1} s^{-1} with the equilibrium constant K_{R1a} (300 K) ~ 10^{-21} cm^3 molecule^{-1} to obtain $k_{R\text{-}1a}$ ~ 10^{11} s^{-1}. This value of $k_{R\text{-}1a}$ is several orders of magnitude higher than k_{R1b} ~ 10^6 s^{-1} at 300 K. k_{R1b} is calculated using the conventional transition state theory. This is a pre-equilibrium case where the reactants and the pre-reactive complex (RC) equilibrate rapidly. Consequently, the equilibrium is virtually not affected by reaction (R1b). Furthermore, we note that no discernible pressure dependence was observed for similar reaction systems we have studied earlier.[11,23] The shallowness of the wells for these pre-reactive complexes are comparable. That being said, the rate coefficients of such complex-forming bimolecular reactions are in the high-pressure limit. In such a scenario, canonical transition state theory (TST) and equilibrium statistical thermodynamics can be applied for kinetic analysis. Therefore, eqn (3) can be employed to obtain the overall rate coefficients for Br atom reactions with the xylenes in a reasonable approximation.

For the reasons discussed above, we chose to employ G4 energetics and molecular parameters to compute the rate coefficients for the xylenes + Br reactions. For our calculations, the low-lying torsional modes of the methyl rotors were treated as a free rotor or a hindered rotor. The torsional modes corresponding to the vibrational wavenumbers ($\nu_i \leq 50$ cm^{-1}) were treated as free rotors. The internal rotation of the $-CH_3Br$ group of the TSs corresponds to a harmonic frequency of >500 cm^{-1}. Therefore, this vibrational mode of the TS can safely be treated as a harmonic oscillator. For all cases, a small adjustment of the barrier height of the G4 energetics, *i.e.* lowering the TS by $\leq$1.5 kJ mol^{-1} in each case, gave overall rate coefficients that are in excellent agreement with the experimental values (see Fig. 3). For the reactions of *m*- and *p*-xylenes with Br, CCSD(T)/cc-pV(D,T)Z//MP2/aug-cc-pVDZ parameters also yielded overall rate coefficients that are in excellent agreement with the experimental data. For these calculations also, we lowered the barrier height by $\leq$1.5 kJ mol^{-1}. However, for the *o*-xylene + Br reaction, similar adjustment of the barrier height of the CCSD(T)/cc-pV(D,T)Z//MP2/aug-cc-pVDZ level of theory yielded rate coefficients that are roughly 50% lower than the experimental data. Further adjustment of the barrier height (lowering by 2 kJ mol^{-1}) resulted in a weak *T*-dependence of the rate coefficients in contrast to the trend shown by the

experimental data. Note that our experiments did not show any significant differences for the reactivity of Br atoms with the *o*- and *p*-isomers of the xylenes. Similarly, theory also did not reveal any difference in the barrier heights of these reactions for a given *ab initio* method (see Fig. 4). That being said, the discrepancy here clearly stems from an entropic effect resulting in a lower value of the pre-exponential factor for the *o*-xylene + Br reaction. For this reaction, MP2/aug-cc-pVDZ parameters yielded a large negative entropy of activation ($\Delta S^{\ddagger} = -487.3$ J K^{-1} mole^{-1} at 300 K) as opposed to $\Delta S^{\ddagger} = -478.3$ J K^{-1} mole^{-1} at 300 K from B3LYP/6-31G(2df,p) molecular parameters in the G4 method. The latter value matches excellently with that from both the MP2/aug-cc-pVDZ and B3LYP/6-31G(2df,p) levels of theory for the *p*-xylene + Br reaction ($\Delta S^{\ddagger} = -478.8$ J K^{-1} mole^{-1} at 300 K). As a result, G4 parameters with a barrier height lowered by $\leq$1.5 kJ mol^{-1} yielded rate coefficients for the xylenes + Br reactions that captured the experimental data remarkably well. Large imaginary frequencies from the MP2 method favoured quantum tunneling which caused severe curvature in the Arrhenius behavior of the xylenes + Br reactions. Therefore, we conclude that the G4 method accurately describes the kinetics and thermochemistry of the xylenes + Br reactions, which may also be appropriate to explore the reactions of other aromatic hydrocarbons with Br. The calculated values of the equilibrium constant (K_{R1a}), rate coefficients (k_{R1b}) and overall rate coefficients [$k_{ov.}(T) = K_{R1a}(T) \times k_{R1b}(T)$] are compiled in Tables S8 and S9 of ESI.†

4. Conclusions

In this study, we have investigated the kinetics of the reactions of atomic bromine with the xylenes over the temperature range of 295 K to 346 K at several concentrations of oxygen using a Pyrex chamber equipped with fluorescent lamps. Additionally, we employed various *ab initio*/statistical rate theory methods to fully characterize the xylenes + Br reaction system. This is the first combined experimental and theoretical study of the kinetics of the reactions of Br atoms with the xylenes. Our findings are summarized below.

(1) The reactions of Br atoms with the xylenes show no dependence on the oxygen concentration. The rate coefficients for the reactions of Br with the xylenes show a weak temperature dependence indicating small but measurable activation energies. The values of the activation energies of these reactions are identical within their experimental uncertainties.

(2) The potential energy surfaces for the reactions of Br atoms with the xylenes were computed using various *ab initio* methods. Several reaction pathways were characterized. However, only the hydrogen abstraction reaction at the methyl site of the xylenes is of kinetic relevance.

(3) Like other Br atom reactions with VOCs, the reactions of Br atoms with the xylenes are found to proceed *via* a complex forming mechanism in an overall endothermic process. The reaction complexes are found at both the entrance and exit channels. The relative stability of the pre-reactive complex is similar to that seen in the complexes of Br/Cl/OH + oxygenated VOCs.

(4) Among the *ab initio* methods employed here, G4 performs the best to quantitively describe the energetic picture of the reactions of Br with the xylenes. A similar observation was made in another study involving the reaction of toluene with Br.[9] G4 values of the standard enthalpies of reaction and standard enthalpies of formation of the xylenes and their radicals agree excellently with the available literature data. Our findings indicate that the G4 method can provide a quantitative kinetic and thermodynamic picture for the reactions of Br atoms with other aromatic hydrocarbons. Of course, this will need further confirmation with future studies involving the reactions of Br atoms with other aromatics such as phenols, aromatic -amines, -esters, -carboxylic acids, -ketones and -aldehydes. For these aromatics + Br reactions, hydrogen bonding may be involved which may significantly alter the topography of the PES from that of the reactions of Br with methyl-substituted benzenes.

(5) With a small adjustment of $\leq$1.5 kJ mol^{-1} in the G4 barrier height of the transition states, the calculated overall rate coefficients are found to agree excellently with the experimental data. The theoretical rate coefficients can be best described by the following three-parameter Arrhenius expressions from 200 to 500 K (in units of cm^3 molecule^{-1} s^{-1}):

$$k_{ov.}[o\text{-}C_6H_4(CH_3)_2 + Br \rightarrow o\text{-}C_6H_4CH_3CH_2 + HBr] = 1.08 \times 10^{-19}\, T^{2.635} \exp(-430.6\ K/T)$$

$$k_{ov.}[m\text{-}C_6H_4(CH_3)_2 + Br \rightarrow m\text{-}C_6H_4CH_3CH_2 + HBr] = 2.44 \times 10^{-20}\, T^{2.856} \exp(-621.9\ K/T)$$

$$k_{ov.}[p\text{-}C_6H_4(CH_3)_2 + Br \rightarrow p\text{-}C_6H_4CH_3CH_2 + HBr] = 7.64 \times 10^{-20}\, T^{2.788} \exp(-599.7\ K/T)$$

It is instructive to compare the relations above, derived from theory, with those reported earlier which were obtained by a conventional linear least squares fit of the experimentally measured rate coefficients to an Arrhenius function without reference to theory. To facilitate this comparison, the logarithmic expressions presented earlier for the *T*-range of 295–346 K are converted below to their non-logarithmic forms.

$$k(T)\cdot[o\text{-}C_6H_4(CH_3)_2 + Br \rightarrow o\text{-}C_6H_4CH_3CH_2 + HBr] = 9.29 \times 10^{-11} \exp(-2121\ K/T)$$

$$k(T)\cdot[m\text{-}C_6H_4(CH_3)_2 + Br \rightarrow m\text{-}C_6H_4CH_3CH_2 + HBr] = 1.65 \times 10^{-11} \exp(-1812\ K/T)$$

$$k(T)\cdot[p\text{-}C_6H_4(CH_3)_2 + Br \rightarrow p\text{-}C_6H_4CH_3CH_2 + HBr] = 1.04 \times 10^{-10} \exp(-2202\ K/T)$$

As above, the units of the rate coefficients are cm^3 molecule^{-1} s^{-1}. The combination of limits on the precision achievable in experimental kinetic measurements and the limited range of temperatures accessible in most kinetic experiments using a single experimental approach generally make

fitting to a three parameter function of temperature difficult. The T^n term often has a comparable influence to the exponential term which can make it hard to obtain an independent and objective fit to both terms. A simple analysis as a function of temperature of the difference between the experimental rate coefficients and those calculated from the two parameter and three parameter fits leads to the following observations.

Over our experimentally accessible range of temperature, the magnitudes of the deviations of the experimental rate coefficients from those calculated from both the two-parameter and three-parameter fits are comparable. The deviations from the two-parameter fit are distributed randomly as a function of temperature, as might be expected for line of best fit parameters obtained by a least squares analysis of experimental data. The deviations from the three-parameter function derived from theory are largest and positive at the lowest temperatures, decreasing steadily with increasing temperature to become negative at the highest temperatures. This behaviour is found for all three xylene isomers. While one might conclude from this that the three-parameter fit has a tendency to overestimate the rate coefficients at low temperatures and underestimate them at high temperatures, the effect is small in our temperature range, approximately 290 K to 350 K. Measurements of the rate coefficients over a much wider temperature range using other experimental approaches would be needed to determine whether this effect is empirical, as a result of the modest range of magnitudes of the rate coefficients, or a result of the method chosen to represent the temperature dependence of the rate coefficients. It might be marginally preferable to use rate coefficients calculated from the two-parameter fit at temperatures that fall within the range 290 K to 350 K since the deviations of the experimental data from the line of best fit are distributed randomly. This temperature range should be adequate for tropospheric chemistry. However, at temperatures significantly above or below this range the three parameter fit is likely to be preferable because it is derived from a theoretical analysis which includes features such as quantum tunneling. For that reason, use of rate coefficients calculated from the two parameter fit should be used with caution when examining chemistry at high temperatures or in regions of the atmosphere above the troposphere.

(6) Our experiments were all made under conditions at which no pressure dependence was detected. We conclude from this that the reactions investigated were in their high pressure limits. The pressures used in our experiments ranged from 101 kPa to 27 kPa. The rate coefficients calculated from our work should therefore be applicable at the pressures encountered in the troposphere. However, considering the molecular complexity of the pre-reactive complexes of the xylenes + Br reaction system, the overall rate coefficients should be at the high-pressure limit for pressures as low as few torr. With the increase of molecular complexity *i.e.* no. of vibrational degrees of freedom, the falloff regime is significantly shifted towards the lower total pressures according to unimolecular rate theory.

Conflicts of interest

The authors declare no conflicts of interest.

Acknowledgements

Research reported in this work was funded by King Abdullah University of Science and Technology (KAUST). This research was also supported by the European Union and the Hungarian State, co-financed by the European Regional Development Fund in the framework of the GINOP-2.3.4-15-2016-00004 project, aimed to promote the cooperation between the higher education and the industry. Further support has been provided by the National Research, Development and Innovation Fund (Hungary) within the TKP2021-NVA-14 project. The experimental work was supported by Acadia University and by the Natural Sciences and Engineering Research Council of Canada.

References

1 B. J. Finlayson-Pitts, *Int. J. Chem. Kinet.*, 2019, **51**, 736–752.
2 B. F. Pitts and J. N. Pitts, *Chemistry of the Upper and Lower Atmosphere: Theory, Experiments and Applications*, Academic Press, New York, NY, 2000.
3 M. R. McGillen, W. P. L. Carter, A. Mellouki, J. J. Orlando, B. Picquet-Varrault and T. J. Wallington, *Earth Syst. Sci. Data Discuss.*, 2020, pp. 1–24.
4 J. A. Manion, R. E. Huie, R. D. Levin, D. R. Burgess Jr., V. L. Orkin, W. Tsang, W. S. McGivern, J. W. Hudgens, V. D. Knyazev, D. B. Atkinson, E. Chai, A. M. Tereza, C.-Y. Lin, T. C. Allison, W. G. Mallard, F. Westley, J. T. Herron, R. F. Hampson and D. H. Frizzell, NIST Chemical Kinetics Database, NIST Standard Reference Database 17, *Version 7.0 (Web Version)*, Release 1.6.8, Data version 2015.09, National Institute of Standards and Technology, Gaithersburg, Maryland, 20899–8320. Web address: http://kinetics.nist.gov, accessed on January 19, 2022.
5 M. Ammann, R. Cox, J. Crowley *et al.*, IUPAC Task Group on Atmospheric Chemical Kinetic Data Evaluation, 2016.
6 R. Atkinson, D. Baulch and R. Cox, *et al.*, Evaluated kinetic and photochemical data for atmospheric chemistry: volume II gas phase reactions of organic species, *Atmos. Chem. Phys.*, 2006, **6**, 3625–4055.
7 B. R. Giri, J. M. Lo, J. M. Roscoe, A. B. Alquaity and A. Farooq, *J. Phys. Chem. A*, 2015, **119**, 933–942.
8 B. R. Giri, J. M. Roscoe, N. González-García, M. Olzmann, J. M. Lo and R. A. Marriott, *J. Phys. Chem. A*, 2011, **115**, 5105–5111.
9 B. R. Giri, J. M. Roscoe, M. Szőri and A. Farooq, *Int. J. Chem. Kinet.*, 2021, **53**, 390–402.
10 J. M. Lo, R. A. Marriott, B. R. Giri, J. M. Roscoe and M. Klobukowski, *Can. J. Chem.*, 2010, **88**, 1136–1145.
11 B. R. Giri, J. M. Roscoe, N. González-García and M. Olzmann, *J. Phys. Chem. A*, 2010, **114**, 291–298.
12 J. T. Jodkowski, M.-T. Rayez, J.-C. Rayez, T. Bérces and S. Dóbé, *J. Phys. Chem. A*, 1998, **102**, 9230–9243.

13 J. T. Jodkowski, M.-T. Rayez, J.-C. Rayez, T. Bérces and S. Dóbé, *J. Phys. Chem. A*, 1999, **103**, 3750–3765.
14 B. R. Giri, F. Khaled, M. Szőri, B. Viskolcz and A. Farooq, *Proc. Combust. Inst.*, 2017, **36**(1), 143–150.
15 R. J. Shannon, M. A. Blitz, A. Goddard and D. E. Heard, *Nat. Chem.*, 2013, **5**, 745.
16 L. G. Gao, J. Zheng, A. Fernández-Ramos, D. G. Truhlar and X. Xu, *J. Am. Chem. Soc.*, 2018, **140**, 2906–2918.
17 K. Imrik, G. Kovács, I. Fejes, I. Szilágyi, D. Sarzyński, S. Dóbé, T. Bérces, F. Márta and J. Espinosa-García, *J. Phys. Chem. A*, 2006, **110**, 6821–6832.
18 B. Ballesteros, A. Ceacero-Vega, A. Garzon, E. Jimenez and J. Albaladejo, *J. Photochem. Photobiol. A*, 2009, **208**, 186–194.
19 B. Joalland, Y. Shi, A. D. Estillore, A. Kamasah, A. M. Mebel and A. G. Suits, *J. Phys. Chem. A*, 2014, **118**, 9281–9295.
20 P. Gupta and B. Rajakumar, *J. Phys. Chem. A*, 2019, **123**, 10976–10989.
21 W. J. Frazee and J. M. Roscoe, *Int. J. Chem. Kinet.*, 2019, **51**, 579–589.
22 B. R. Giri and J. M. Roscoe, *J. Phys. Chem. A*, 2010, **114**, 8369–8375.
23 B. R. Giri and J. M. Roscoe, *J. Phys. Chem. A*, 2009, **113**, 8001–8010.
24 M. Wheeler, R. Mills and J. M. Roscoe, *J. Phys. Chem. A*, 2008, **112**, 858–865.
25 A. Ryzhkov, P. Ariya, F. Raofie, H. Niki and G. Harris, *Adv. Quantum Chem.*, 2008, **55**, 275–295.
26 A. Bierbach, I. Barnes and K. Becker, *Atmos. Environ.*, 1999, **33**, 2981–2992.
27 R. Atkinson and J. Arey, *Chem. Rev.*, 2003, **103**, 4605–4638.
28 D. Mehta, A. Nguyen, A. Montenegro and Z. Li, *J. Phys. Chem. A*, 2009, **113**, 12942–12951.
29 A. Galano and J. Raúl Alvarez-Idaboy, in *Advances in Quantum Chemistry*, ed. E. G. Michael and S. J. Matthew, Academic Press, 2008, vol. 55, pp. 245–274.
30 J. R. Alvarez-Idaboy, N. Mora-Diez, R. J. Boyd and A. Vivier-Bunge, *J. Am. Chem. Soc.*, 2001, **123**, 2018–2024.
31 L. A. Curtiss, K. Raghavachari, P. C. Redfern, V. Rassolov and J. A. Pople, *J. Chem. Phys.*, 1998, **109**, 7764–7776.
32 L. A. Curtiss, P. C. Redfern and K. Raghavachari, *J. Chem. Phys.*, 2007, **126**, 084108.
33 C. Møller and M. S. Plesset, *Phys. Rev.*, 1934, **46**, 618–622.
34 A. D. Becke, *J. Chem. Phys.*, 1992, **96**, 2155–2160.
35 A. D. Becke, *J. Chem. Phys.*, 1996, **104**, 1040–1046.
36 A. D. Becke, *J. Chem. Phys.*, 1997, **107**, 8554–8560.
37 A. K. Wilson, D. E. Woon, K. A. Peterson and T. H. D. Jr, *J. Chem. Phys.*, 1999, **110**, 7667–7676.
38 T. H. Dunning, *J. Chem. Phys.*, 1989, **90**, 1007.
39 R. D. Johnson, *NIST computational chemistry comparison and benchmark database (CCCBDB)*, Vol. NIST Standard Reference Database Number 101 Release 17b, 2015.
40 K. Fukui, *Acc. Chem. Res.*, 1981, **14**, 363–368.
41 G. D. Purvis and R. J. Bartlett, *J. Chem. Phys.*, 1982, **76**, 1910–1918.
42 G. E. Scuseria and H. F. Schaefer, *J. Chem. Phys.*, 1989, **90**, 3700.
43 J. A. Pople, M. Headgordon and K. Raghavachari, *J. Chem. Phys.*, 1987, **87**, 5968–5975.
44 J. M. Martin, *Chem. Phys. Lett.*, 1996, **259**, 669–678.
45 D. Feller and D. A. Dixon, *J. Chem. Phys.*, 2001, **115**, 3484–3496.
46 R. A. Kendall, T. H. Dunning and R. J. Harrison, *J. Chem. Phys.*, 1992, **96**, 6796.
47 T. J. Lee and P. R. Taylor, *Int. J. Quantum Chem.*, 1989, 199–207.
48 B. Ruscic and D. H. Bross, *Active Thermochemical Tables (ATcT) values based on ver. 1.122r of the Thermochemical Network*, 2021, available at ATcT.anl.gov.
49 E. Goos, A. Burcat and B. Ruscic, Extended Third Mellennium Thermodynamic Database of New NASA Polynomials with Active Thermochemical Tables Update, available from http://garfield.chem.elte.hu/Burcat/NEWNASA.TXT.
50 M. J. Frisch, G. W. Trucks, H. B. Schlegel, G. E. Scuseria, M. A. Robb *et al.*, *Gaussian 09 Revision D.01*, Gaussian, Inc., Wallingford CT, 2009.
51 S. L. Glasstone and K. J. H. Eyring, *The Theory of Rate Processes*, McGraw-Hill, New York, 1941.
52 J. I. Steinfeld, *Chemical kinetics and dynamics*, 2nd edn, Prentice Hall, Upper Saddle River, NJ, 1999.
53 D. A. McQuarrie, *Statistical Thermodynamics*, University Science Books, Mill Valley, CA, 1973.
54 C. Malcolm, NIST-JANAF, Thermochemical Tables-Fourth Edition. J. Phys. Chem. Ref. Data, 1998, Monograph No. 9.
55 J. R. Barker, T. L. Nguyen, J. F. Stanton *et al.*, Multiwell-2017 Software Suite, 2017.
56 O. Kondo and S. W. Benson, *Int. J. Chem. Kinet.*, 1984, **16**, 949–960.
57 C. Fan, W. Wang, B. Shi, Y. Chen, K. Wang, W. Zhang, Z. Sun and M. Ge, *J. Phys. Chem. A*, 2020, **124**, 721–730.
58 J. C. Hansen and J. S. Francisco, *ChemPhysChem*, 2002, **3**, 833–840.
59 I. W. Smith and A. Ravishankara, *J. Phys. Chem. A*, 2002, **106**, 4798–4807.
60 K. P. Somers and J. M. Simmie, *J. Phys. Chem. A*, 2015, **119**, 8922–8933.
61 C. Sosa and H. Bernhard Schlegel, *Int. J. Quantum. Chem.*, 1986, **29**, 1001–1015.
62 A. Montoya, T. N. Truong and A. F. Sarofim, *J. Phys. Chem. A*, 2000, **104**, 6108–6110.
63 J. Cioslowski, G. Liu, M. Martinov, P. Piskorz and D. Moncrieff, *J. Am. Chem. Soc.*, 1996, **118**, 5261–5264.
64 J. A. Pople, P. M. Gill and N. C. Handy, *Int. J. Quantum Chem.*, 1995, **56**, 303–305.
65 J. F. Stanton, *J. Chem. Phys.*, 1994, **101**, 371–374.
66 A. S. Menon and L. Radom, *J. Phys. Chem. A*, 2008, **112**, 13225–13230.
67 E. Prosen, W. Johnson and F. Rossini, *J. Res. Natl. Bur. Stand.*, 1946, **36**, 455–461.